Elastic Properties of Cu–Co Multilayers

JOHN R. DUTCHER, SUKMOCK LEE, CRAIG D. ENGLAND, GEORGE I. STEGEMAN and CHARLES M. FALCO

Optical Sciences Center and Department of Physics, University of Arizona, Tucson, AZ 85721 (U.S.A.)

(Received April 21, 1989)

Abstract

The acoustic phonon modes of sputter-deposited Cu–Co multilayers were studied using Brillouin scattering. These are the first such measurements to be made on an f.c.c.–f.c.c. multilayer system. The multilayer samples had a fixed atomic percentage of cobalt (53 at.%). The effective elastic constants of the multilayer samples, which were obtained by comparing the data with calculated dispersion curves for the phonon modes, were independent of the multilayer modulation wavelength.

1. Introduction

There has been considerable recent interest in the elastic properties of metallic multilayers and superlattices. Reports of large enhancements of the biaxial modulus (the "supermodulus effect") for metallic multilayers near a multilayer modulation wavelength value of 2.5 nm [1, 2] have sparked both theoretical [3–5] and experimental studies [6–8]. To date, Brillouin scattering has been used to study the elastic properties of Cu–Nb [6, 9], Mo–Ni [10], V–Ni [11], Mo–Ta [7], Fe–Pd [12] and Au–Cr [13] multilayers. In contrast with reported enhancements of the biaxial modulus, many of these multilayer systems exhibited a minimum in one or more of the elastic constants near a modulation wavelength value of 2.5 nm. However, all these metal combinations are b.c.c.–f.c.c. with the exception of Mo–Ta which is b.c.c.–b.c.c., whereas the enhancement of the biaxial modulus has been reported only in f.c.c.–f.c.c. multilayers [1, 2]. In this paper we present the first Brillouin scattering studies of an f.c.c.–f.c.c. multilayer system: Cu–Co.

Brillouin scattering from the thermally excited acoustic phonon modes of a supported film is an excellent technique for measuring the elastic constants of the film [14]. Laser light of wavelength λ is directed onto the sample surface and a small fraction of the light is inelastically scattered from the phonon modes of the film. For metallic films, the light interacts primarily with the Rayleigh and Sezawa surface acoustic phonon modes via the surface ripple mechanism [15]. The atomic displacements perpendicular to the sample surface deform or ripple the surface and these displacements couple to the electric field of the incident optical radiation to produce scattered light with frequencies shifted from the incident light frequency by the phonon mode frequency. Typically, in a Brillouin backscattering experiment, the frequencies f of the phonon modes are measured as a function of the angle θ between the incident laser light and the sample normal. The data are usually presented as dispersion curves with the phonon mode velocities v plotted as a function of the product of the in-plane wavevector component $q=(4\pi/\lambda)\sin\theta$ and the thickness of the film h, where $v=2\pi f/q$.

2. Experimental details

The growth and X-ray characterization of the Cu–Co multilayer samples has been described in detail by England *et al.* [16]. The samples were grown by alternately depositing layers of copper and cobalt on single-crystal sapphire substrates using magnetically enhanced d.c. triode sputtering techniques. The copper layers grew in the f.c.c. structure with strong [111] texture for both copper single-layer films and Cu–Co multilayer films. Cobalt single-layer films that were 96.1 and 293 nm thick grew in the h.c.p. structure with strong [100] and [002] texture. However, in the multilayer samples for which the cobalt layer thicknesses were less than 5.5 nm, the cobalt layers grew in the f.c.c. structure with strong [111] texture. The structure of the cobalt layers was inferred from the average lattice spacing d_{av} of

0921-5093/90/$3.50

the multilayer samples along the growth direction. The value of d_{av} was calculated from the position of the (111) X-ray diffraction peak near $2\theta = 43°$, as measured using a Bragg–Brentano diffractometer, and was essentially constant for the entire set of Cu–Co multilayers: $d_{av} = 0.2066 \pm 0.0004$ nm. The coherence length along the growth direction, obtained from the (111) X-ray diffraction peak linewidths using the Scherrer equation [17], was typically 17 nm. This coherence length value is considerably smaller than the value of 30–40 nm obtained for Mo–Ta multilayers [18]. The multilayer samples had a fixed atomic percentage of cobalt (53 at.%), with modulation wavelengths Λ ranging from 0.87 to 10.8 nm. The number of Cu–Co bilayers in the multilayer samples was chosen to give a total film thickness h of approximately 110 nm, with the exception of the multilayer with $\Lambda = 8.97$ nm for which the film thickness was 25% higher. Single-layer films of copper ($d_{Cu} = 94.0$ nm) and cobalt ($d_{Co} = 105$ nm) were also measured. The thicknesses of the single-layer and multilayer films were determined to within $\pm 3\%$ using Rutherford backscattering (RBS) [16].

The Brillouin scattering measurements were performed in air at room temperature. 100 mW of laser light ($\lambda = 5145$ Å), polarized in the plane of incidence, was focused onto the sample surface. 180° backscattered light, also polarized in the plane of incidence, was collected and analyzed using a high contrast tandem (3+3 passes) Fabry–Perot interferometer which has been described elsewhere [19, 20]. Since only the polarized scattering was collected, the depolarized scattering from thermally excited magnetic waves [20] present in the cobalt layers was not observed in the Brillouin scattering spectra. For each sample, data were collected for six different angles of incidence θ within the range from $\theta = 22°$ to $\theta = 70°$. A typical data collection time for each spectrum was 2 h.

For all the Brillouin scattering measurements, a lens with a 50 mm focal length and an f number of 1.4 was used to collect the scattered light. A slit was placed in the center of the scattered beam to limit the spread in the scattering wavevector. The slit width was a quarter of the diameter of the scattered beam. For $\theta < 30°$, the Rayleigh mode frequency is very small (7 GHz or less) and the peak in the Brillouin spectrum occurs very close to the large elastic scattering peak with zero frequency shift. The purpose of the slit is to reduce the instrumental linewidth for small angles of incidence θ, *e.g.* for $\theta = 22°$; the linewidth was reduced by a factor of 2 for the multilayer sample with $\Lambda = 8.24$ nm. The narrower linewidth should allow more accurate determination of the Rayleigh mode velocity. In addition, it is important to limit the range of scattering wavevectors for small angles of incidence because the light scattering cross-section for the surface ripple mechanism depends strongly on θ for $\theta < 30°$ (see for example Fig. 6 of ref. 21). The large variation in collected intensity across the collection aperture for low values of θ can lead to false shifts in the measured mode frequencies. However, in the present case, the difference between the measured Rayleigh mode velocities with and without the slit placed in the scattered beam for the multilayer sample with $\Lambda = 8.24$ nm and $\theta = 22°$ was comparable with the uncertainty in the velocity measurement (about 2%).

3. Results and discussion

A typical Brillouin scattering spectrum for the multilayer sample with $\Lambda = 8.24$ nm is shown in Fig. 1. The total data collection time for this spectrum was 2.05 h. The spectrum consists of a series of peaks symmetric about zero frequency shift corresponding to light scattering from the Rayleigh and Sezawa acoustic modes. The strongest of these peaks with the smallest non-zero frequency shift arises from light scattering

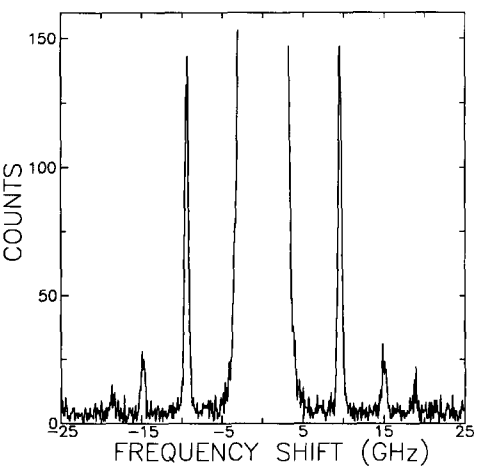

Fig. 1. Brillouin scattering spectrum for the multilayer sample with modulation wavelength $\Lambda = 8.24$ nm and a total film thickness $h = 115.4$ nm. The spectrum was collected using an incidence angle θ of 70° and an incident laser power of 100 mW. The total counting time for the spectrum was 2.05 h.

from the Rayleigh mode. The smaller peaks with larger frequency shifts correspond to light scattering from the Sezawa modes of the film. Typically, two modes were observed for small angles of incidence and three modes were observed for large angles of incidence. The number of observed modes is small compared with previous Brillouin scattering measurements on Mo–Ta [7] and Cu–Nb [9] because the total film thickness of the Cu–Co films is smaller and the number of observed modes varies inversely with the thickness. The small number of observed modes does not indicate that the quality of the Cu–Co samples is poorer than that of the Mo–Ta and Cu–Nb samples. For all single-layer and multilayer samples, the natural linewidths of the modes due to phonon damping processes were assumed to be small compared with the instrumental linewidth of each peak. The measured mode frequencies were independent of the propagation direction in the plane of the samples.

The measured dispersion of the Rayleigh and first two Sezawa mode velocities for all the multilayer samples are shown in Fig. 2. For a given qh value, only small variations were observed in the measured Rayleigh mode velocities v_R and the Sezawa mode velocities $v_{S,i}$ for the entire series of multilayer samples, *e.g.* $v_R = 2680 \pm 130$ m s^{-1} and $v_{S,1} = 4160 \pm 90$ m s^{-1} for $qh = 2.34$.

For the analysis of the elastic properties, we treated each multilayer sample as a single film with one set of effective elastic constants and

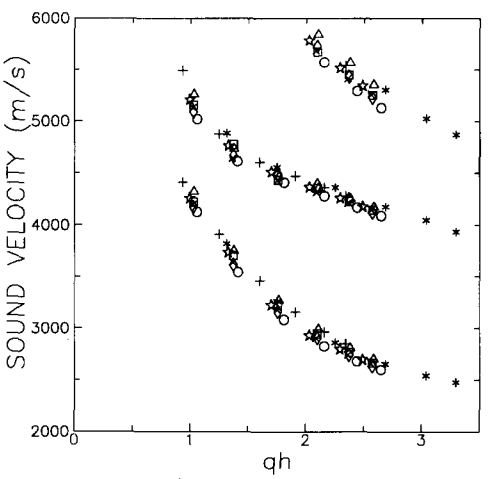

Fig. 2. Dependence of the measured velocities of sound on the product of the in-plane wavevector q and the film thickness h for each of the multilayer samples: ×, $\Lambda = 0.872$ nm; +, $\Lambda = 1.70$ nm; □, $\Lambda = 3.03$ nm; ◇, $\Lambda = 4.31$ nm; △, $\Lambda = 5.63$ nm; ○, $\Lambda = 8.24$ nm; *, $\Lambda = 8.97$ nm; ☆, $\Lambda = 10.8$ nm.

calculated the acoustic mode velocities of the single supported film using the procedure of Farnell and Adler [22]. To simplify the calculation of the dispersion curves, we approximated the symmetry of the sapphire substrate, which is actually trigonal, as hexagonal with elastic constants $c_{11,s} = 494$ GPa, $c_{13,s} = 114$ GPa, $c_{33,s} = 496$ GPa and $c_{44,s} = 145$ GPa. In this approximation, which has been used previously [12], the small c_{14} ($= -23$ GPa) term is set equal to zero. The symmetry of the single-layer and multilayer films was assumed to be hexagonal with the c axis normal to the film plane. During the sputter deposition process, the crystallites tend to grow with a particular crystal direction (the texture direction) perpendicular to the film plane and with random orientation within the plane. This process yields films that are elastically isotropic in the film plane on a macroscopic scale, which is equivalent to hexagonal symmetry with the c axis normal to the film plane [23]. The dispersion of the Rayleigh and Sezawa modes of a supported film of hexagonal symmetry is determined by four of the five independent elastic constants: c_{11}, c_{13}, c_{33} and c_{44}. The remaining independent elastic constant c_{12} affects the dispersion of Love waves which have displacements that are perpendicular to the sagittal plane. Love waves have been observed in Cu–Nb multilayers using Brillouin scattering [24].

The elastic constants for each single-layer and multilayer sample were obtained using a least-squares fitting procedure. The data obtained for six different angles of incidence were successively fitted to models with isotropic, cubic and hexagonal symmetry with two, three and four independent elastic constants respectively.

The initial elastic constant values for the fitting procedure for the single-layer films were taken to be the averages of the Voigt and Reuss bulk-based estimates [25] listed in Table 1 for copper and cobalt crystallites with [111] texture. The resulting best-fit hexagonal elastic constants for the copper and cobalt single-layer films are also listed in Table 1. The best-fit values for the copper film are considerably lower than those estimated from the bulk copper elastic constants [26], while the best-fit values for the cobalt film are considerably higher than those estimated from the bulk cobalt elastic constants [26] for both f.c.c. and h.c.p. cobalt. Similar discrepancies between the measured mode velocities and those calculated using the elastic constants of the bulk

TABLE 1 Elastic constant values for the copper and cobalt single-layer films and a representative multilayer sample

	c_{11}	c_{12}	c_{13}	c_{33}	c_{44}
Cu single layer					
Bulk f.c.c. estimate[a]	202	106	103	205	45
Best fit	149	—	65	125	38
Co single layer					
Bulk f.c.c. estimate[a]	298	134	129	303	78
Bulk h.c.p.	295	159	111	335	71
Best fit	412	—	267	364	61
Cu–Co multilayer ($\Lambda = 8.24$ nm)					
Bulk (f.c.c. Cu–f.c.c. Co) estimate[b]	252	120	114	248	58
Bulk (f.c.c. Cu–h.c.p. Co) estimate[b]	251	134	106	258	56
Single-layer estimate[c]	246	—	121	192	48
Best fit[d]	267	—	138	198	48
Best fit[e]	269	—	144	210	47

[a]Effective hexagonal elastic constants obtained from the bulk cubic elastic constants (c axis along [111]).
[b]Estimated multilayer elastic constants [27] based on the effective hexagonal elastic constants for the bulk materials.
[c]Estimated multilayer elastic constants [27] based on the best-fit elastic constants for the single layer films of copper and cobalt.
[d]Best fit with c_{11}, c_{13}, c_{33}, and c_{44} as free parameters.
[e]Best fit with c_{33} and c_{44} as free parameters and with c_{11} and c_{13} values fixed to average multilayer values.

metals have been observed previously by Bell *et al.* [9] for copper and niobium single-layer films. Bell *et al.* also found that a deliberately introduced fivefold increase in the oxygen contamination of the Cu–Nb multilayer films, as described using RBS, resulted in an increase of c_{44} by about 9%. It is possible that the differences between the bulk-based estimates and the best-fit values of the elastic constants for the copper and cobalt single-layer films are due to impurities incorporated into the films during the sputter deposition process. Unfortunately, the oxygen content of the Cu–Co films could not be measured using RBS since these samples were grown on sapphire, an oxygen-containing compound (Al_2O_3).

The superlattice effective elastic constants [27] calculated using the best-fit elastic constant values for the single-layer films were used as the initial values for the fitting procedure for the multilayer films. The multilayer hexagonal elastic constants obtained using the "successive fitting" procedure described above were the same as those obtained by fitting the data directly to a model with hexagonal symmetry. A further indication of the validity of our fitting procedure was the small variation (10% or less) in each of the best-fit hexagonal elastic constant values for the entire series of multilayer samples. A small variation was expected because of the small spread (less than 5%) in the measured Rayleigh mode velocities and Sezawa mode velocities for the entire series of multilayer samples for a given qh value (see Fig. 2).

Although all the best-fit elastic constant values for the multilayer films obtained by varying all four elastic constants were independent of Λ to within 10%, we decided to fit the data with two of the four elastic constants fixed at their average values for all multilayer samples. This approach has been used before [7, 9] to reduce uncertainties introduced into the fitted elastic constant values by the large number of free parameters. In these studies, c_{33} and c_{44} were allowed to vary in the fitting procedure. c_{33} was chosen as a fitting parameter to observe whether there was a Λ-dependent strain normal to the film surface. For the previous studies [7, 9] in which the film thicknesses were large (300–440 nm), the effect of c_{44} on the dispersion curves was decoupled from the effects of the other elastic constants. For large values of qh (≈ 10), the Rayleigh wave velocity v_R is essentially independent of qh, and the c_{44} constant of the film can be determined very accurately from the constant value of v_R. A Λ dependence of c_{44} was observed in Mo–Ta [7] and Cu–Nb [9], and a Λ dependence of the Rayleigh mode velocity was observed in several different metal multilayer systems [6, 10, 11, 13]. For smaller values of qh, such as for the Cu–Co samples (Figs. 2 and 3), c_{44} is not decoupled from the

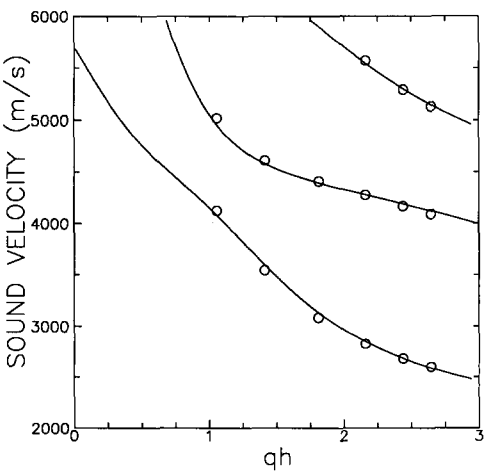

Fig. 3. Dependence of the velocities of sound on the product of the in-plane wavevector q and the total film thickness h for the multilayer sample with modulation wavelength $\Lambda = 8.24$ nm and $h = 115.4$ nm; o, experimental data collected for six different angles of incidence; — —, calculated using the elastic constant values $c_{11} = 269$ GPa, $c_{13} = 144$ GPa, $c_{33} = 210$ GPa and $c_{44} = 47$ GPa.

other elastic constants. Nevertheless, because of the Λ dependence of c_{44} observed for other multilayer systems, we decided to allow c_{44} to vary in our fitting procedure. Since the difference between the lattice constants of f.c.c. copper and f.c.c. cobalt is very small (about 2%), it is expected that the in-plane strains between adjacent layers of the multilayer samples should be very small and that c_{11} should not depend on Λ. The elastic constants c_{11} and c_{13} were fixed at the values of 269 GPa and 144 GPa respectively.

The best-fit elastic constant values for the multilayer samples obtained with two and four free parameters differed by less than 5%. Good agreement (within 15%) was also obtained between the multilayer best-fit elastic constants and those estimated from the best-fit elastic constants of the single-layer films of copper and cobalt. The differences between the multilayer best-fit elastic constants and those estimated from the elastic constants of the bulk metals were larger (up to 30% for c_{33}). However, these larger differences are not surprising since large differences were observed between the best-fit elastic constants and the bulk-based estimates for the single-layer films. A list of the different sets of elastic constant values is given in Table 1 for the multilayer sample with $\Lambda = 8.24$ nm.

The dispersion of the mode velocities for the multilayer sample with $\Lambda = 8.24$ nm is shown in Fig. 3. The full curves were calculated using the values of c_{33} and c_{44} obtained from the fitting procedure with $c_{11} = 269$ GPa and $c_{13} = 144$ GPa. The curves were virtually identical with those calculated using the best-fit elastic constant values with all four constants as free parameters. The measured velocities agree with the velocities calculated from the fit to within 1.5%. The excellent agreement obtained between the data and fitted curves in Fig. 3 is typical of all the multilayer samples, as well as the single-layer films.

The dependence of the elastic constants on the multilayer modulation wavelength Λ is shown in Fig. 4. The error bars indicated in the figure for the elastic constants are primarily due to uncertainties in the film thickness. Therefore, within the error associated with each constant, we find that both c_{33} and c_{44} for this f.c.c.-f.c.c. multilayer system are independent of Λ.

There are two reasons why the absence of a variation in c_{44} as a function of Λ is not surprising. For Mo–Ta multilayers, c_{44} has been shown to have the same qualitative Λ dependence as the

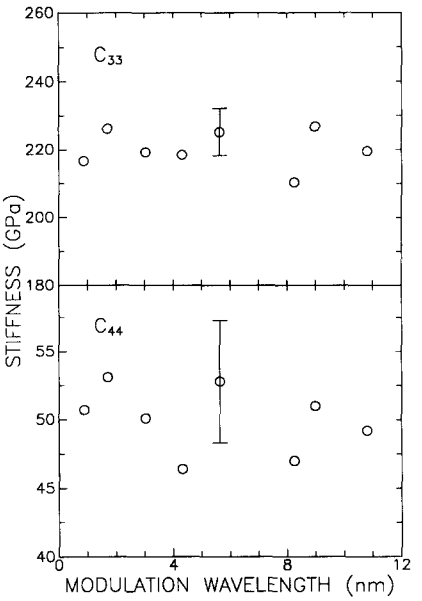

Fig. 4. Modulation wavelength dependence of the c_{33} and c_{44} elastic constants for the Cu–Co multilayer samples. The values of c_{33} and c_{44} were obtained by a least-squares fit of an acoustic model to the data for each sample with $c_{11} = 269$ GPa and $c_{13} = 144$ GPa.

inverse of the average lattice spacing d_{av} along the growth direction [7, 28]. Since d_{av} for the Cu–Co multilayers was constant to within $\pm 0.2\%$, as mentioned in Section 2, we do not expect a Λ-dependent variation in c_{44} for the Cu–Co multilayers. Also, it has been suggested that the size of the variation in c_{44} is directly related to the lattice mismatch between the two metals in the mutlilayer [7]. Because the structure of the copper and cobalt in the multilayer films is the same (f.c.c.) with a very small lattice mismatch (about 2%), we do not expect c_{44} to depend on Λ.

4. Summarizing remarks

We have made precise measurements of the surface acoustic phonon modes for a series of Cu–Co multilayer films with a fixed atomic percentage of cobalt (53 at.%). We have obtained excellent agreement between the measured and calculated mode velocities. The best-fit elastic constants of the multilayer films are significantly different from those estimated from the elastic constants of bulk copper and cobalt and measured single-layer films of copper and cobalt. The elastic constants of the multilayer films are independent of the multilayer modulation wavelength Λ. The absence of Λ-dependent variation in c_{44} seems to be correlated with the absence of a

Λ-dependent variation in the average lattice spacing along the growth direction and with the small lattice mismatch between the two metals.

With the sensitivity now available for determining elastic constants using the Brillouin scattering technique, we are now investigating elastic property anomalies in greater detail for metallic multilayers obtained by sputtering and molecular beam epitaxy to determine the origin of the anomalies in these materials.

Acknowledgments

This work was supported by the Office of Naval Research under Contract N00014-88-K-0298. One of the authors (J.R.D.) is grateful to the Natural Sciences and Engineering Research Council of Canada for a postdoctoral fellowship.

References

1 W. M. C. Yang, T. Tsakalakos and J. E. Hilliard, *J. Appl. Phys., 48* (1977) 876.
2 G. E. Henein and J. E. Hilliard, *J. Appl. Phys., 54* (1983) 728.
3 D. Wolf and J. F. Lutsko, *Phys. Rev. Lett., 60* (1988) 1170.
4 B. W. Dodson, *Phys. Rev. B, 37* (1988) 727.
5 R. C. Cammarata and K. Sieradzki, *Phys. Rev. Lett., 62* (1989) 2005.
6 A. Kueny, M. Grimsditch, K. Miyano, I. Banerjee, C. M. Falco and I. K. Schuller, *Phys. Rev. Lett., 48* (1982) 166.
7 J. A. Bell, W. R. Bennett, R. Zanoni, G. I. Stegeman, C. M. Falco and F. Nizzoli, *Phys. Rev. B, 35* (1987) 4127.
8 B. M. Clemens and G. L. Eesley, *Phys. Rev. Lett., 61* (1988) 2356.
9 J. A. Bell, W. R. Bennett, R. Zanoni, G. I. Stegeman, C. M. Falco and C. T. Seaton, *Solid State Commun., 64* (1987) 1339.
10 M. R. Khan, C. S. L. Chun, G. P. Felcher, M. Grimsditch, A. Kueny, C. M. Falco and I. K. Schuller, *Phys. Rev. B, 27* (1983) 7186.
11 R. Danner, R. P. Huebener, C. S. L. Chun, M. Grimsditch and I. K. Schuller, *Phys. Rev. B, 33* (1986) 3696.
12 P. Baumgart, B. Hillebrands, R. Mock, G. Güntherodt, A. Boufelfel and C. M. Falco, *Phys. Rev. B, 34* (1986) 9004.
13 P. Bissanti, M. B. Brodsky, G. P. Felcher, M. Grimsditch and L. R. Sill, *Phys. Rev. B, 35* (1987) 7813.
14 R. Zanoni, J. A. Bell, G. I. Stegeman and C. T. Seaton, *Thin Solid Films, 154* (1987) 225.
15 R. Loudon, *Phys. Rev. Lett., 40* (1978) 581.
16 C. D. England, W. R. Bennett and C. M. Falco, *J. Appl. Phys., 64* (1988) 5757.
17 H. P. Klug and L. E. Alexander, *X-ray Diffraction Procedures*, 2nd edn., Wiley, New York, 1974, Chapter 9.
18 W. R. Bennett and C. M. Falco, *J. Appl. Phys., 63* (1988) 2176.
19 S. M. Lindsay, M. W. Anderson and J. R. Sandercock, *Rev. Sci. Instrum., 52* (1981) 1478.
20 J. R. Sandercock, in M. Cardona and G. Güntherodt (eds.), *Light Scattering in Solids III*, Springer, Berlin, 1982, Chapter 6.
21 R. Loudon and J. R. Sandercock, *J. Phys. C, 13* (1980) 2609.
22 G. W. Farnell and E. L. Adler, in W. P. Mason and R. N. Thurston (eds.), *Physical Acoustics*, Vol. IX, Academic Press, New York, 1972, Chapter 2.
23 B. A. Auld, *Acoustic Fields and Waves in Solids*, Vol. 1, Wiley, New York, 1973, p. 116.
24 J. A. Bell, R. Zanoni, C. T. Seaton, G. I. Stegeman, W. R. Bennett and C. M. Falco, *Appl. Phys. Lett., 51* (1987) 652.
25 M. J. P. Musgrave, *Crystal Acoustics*, Holden-Day, San Francisco, CA, 1970, p. 177.
26 K. H. Hellwege and A. M. Hellwege (eds.), *Landolt-Börnstein, New Series*, Group 3, Vol. 18, Springer, Berlin, 1984.
27 M. Grimsditch, *Phys. Rev. B, 31* (1985) 6818.
28 J. L. Makous and C. M. Falco, *Solid State Commun., 68* (1988) 375.